

## Correction of Single-Crystal Intensities for Average Values of Multiple Reflection\*

BY Y. LE PAGE AND E. J. GABE

Division of Chemistry, National Research Council of Canada, Ottawa K1A 0R9, Canada

(Received 10 May 1978; accepted 26 June 1978)

### Abstract

For short wavelengths, *Umweganregung* cannot be experimentally eliminated. Its average unscaled intensity for a random orientation of the crystal is  $U(2\theta_1) = \int_{\theta_1, \varphi} (\sin 2\theta / \sin 2\theta_1) P(\theta_1, \theta, \varphi) \exp[-2K(\sin^2 \theta + \sin^2 \theta_{12})] d\theta d\varphi$ , where  $(2\theta, \varphi)$  are the spherical coordinates of a point on the Ewald sphere when the intensity measurement is made at  $(2\theta_1, 0)$ , the angle between the two directions being  $2\theta_{12}$ , while  $K$  is the slope of a plot of  $\ln \langle F(\text{obs}) \rangle$  as a function of  $\sin^2 \theta$ , and  $P(\theta_1, \theta, \varphi)$  is the polarization correction appropriate to the double reflection. Diffraction intensities were measured for epidote and quartz. A plot of  $\langle |F(\text{calc})| \rangle / \langle F(\text{obs}) \rangle$  as a function of  $F(\text{obs})$  for epidote was considerably improved by the subtraction from each intensity measurement of a number of counts  $SU(2\theta_1)$ , where  $S$  is an experimental scale factor while  $U(2\theta_1)$  was calculated for epidote by numerical integration over the Ewald sphere. The refinement residuals for both compounds improved after correction of the intensities and the weights.

### Introduction

The phenomenon of multiple reflection was first observed by Renninger (1937). It has since been studied quantitatively by a number of authors and its detrimental effect on intensity data is well known. Moon & Schull (1964) present a simple theoretical survey of the phenomenon and Coppens (1968) describes a method for avoiding the large contributions of double reflections to measured integrated intensities provided that the indices of the intense reflections are known. Post (1969) and Gabe, Portheine & Whitlow (1973) recognize that multiple reflections systematically increase the weak reflection intensities. The effect is more pronounced in the compounds with low thermal motion.

Critical comparison of quartz intensity measurements (Le Page & Donnay, 1976; Le Page, 1978) and more recent intensity measurements on quartz showed unambiguously that the weak reflection intensities are systematically overestimated even though very few

individual measurements differ from the average of their symmetry-related reflections by amounts sufficient to justify their elimination from the data sets. The magnitude of the effect depends on the sample, on the divergence of the beam and on the data-collection method used. Any single large observed intensity difference from the average of equivalent intensities can be eliminated by rotation about the diffraction vector ( $\psi$ -scanning). When performed on systematic absences, this experiment shows that the effect is rarely absent. Analysis of the refinement results shows that the effect was more pronounced in the small Le Page & Donnay sample than in the larger Le Page sample, using Mo  $K\alpha$  radiation in both cases. It was even smaller when Mo  $K\beta_1$  radiation was used, probably due to the shorter wavelength and the different intensity-measurement method used. Although various effects might contribute to the increasing of the weak intensities, multiple reflection is clearly indicated here by the fact that the measurements are repeatable within counting statistics but are considerably changed by small rotations about the diffraction vector, particularly at low angles.

There are two ways of regarding the phenomenon of multiple reflection: (a) it is an avoidable unwanted effect that should be eliminated from the experiment; (b) it is an unavoidable effect that should be accounted for in the data processing. The first approach is effective for long wavelengths where the number of reciprocal-lattice nodes in diffraction position at any given time is small owing to the smaller size of the Ewald sphere. The method suggested by Coppens (1968) is a suitable way of dealing with the situation in this case. When using a shorter wavelength, however, one is forced to the second approach. With the same beam divergence, the reciprocal volume capable of simultaneous diffraction at a given instant is 10 times larger with Mo  $K\alpha$  radiation than with Cu  $K\alpha$ , while it is nearly 15 times larger when Mo  $K\beta$  is used. For shorter wavelengths, the number of contributing reflections increases but the reflectivity of each of them decreases owing to various factors giving an overall decrease of the effect.

In these circumstances, the multiple-reflection contributions of many reflections add up to give a sizeable and essentially random effect, especially after averaging the symmetry-related reflections. This should be ac-

\* NRC No. 16908.

counted for in the data reduction in two ways: (a) the expected intensity of multiple reflection should be subtracted from each net intensity measurement; (b) the variance of the net intensity should take account of the random aspect of the effect. It is this second approach which will be developed in this paper with no attempt being made to avoid the phenomenon.

### Mechanism of multiple reflections

The mechanism of re-reflection of a wave, whose intensity is being measured, along direction (1) (Fig. 1) of beams initially propagating along other directions (*Umweganregung*) can be described in the following way when the density of nodes in reciprocal space is high. We assume that the crystal is unabsorbing, that the pathlengths of the various beams are equal and that the presence of more than one node in diffraction position does not alter the primary intensities reflected in the corresponding directions. The kinematical model of diffraction is assumed throughout this study.

The volume element cut out of the Ewald sphere by a  $\Delta\theta\Delta\varphi$  increment of the spherical coordinates of the direction  $(2\theta, \varphi)$  contains at a given instant a probable number  $N(2\theta)\Delta\theta\Delta\varphi$  of nodes. The actual number of nodes in the volume element will change but the probable number is proportional to the volume element. Only node 1 need be considered to be moving, because any node leaving the reflection condition will probably be replaced by another node entering it. This will actually improve the averaging because the intensities will in general be different and permit us to consider that the moduli of the structure factors depend on  $2\theta$  only. Each node in this volume element is responsible for a diffracted beam (2) reflected from the incident beam (0) with reflectivity  $r_{02}(2\theta, \varphi)$ . This intensity is re-reflected along beam (1) with average reflectivity  $r_{21}(2\theta, \varphi)$  as long as node 1 satisfies the geometrical condition for re-reflection and the duration of that condition is  $t_{21}(2\theta, \varphi)$ . Therefore, the integrated inten-

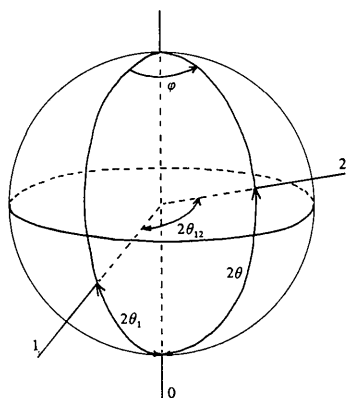


Fig. 1. Definition of the angles used in the calculations.

sity  $Q_1$  is increased by a probable *Umweganregung* contribution  $\Delta Q_1$  equal to:

$$I_o \int_{\theta, \varphi} N(2\theta) r_{02}(2\theta, \varphi) r_{21}(2\theta, \varphi) t_{21}(2\theta, \varphi) d\theta d\varphi.$$

### Evaluation of the individual terms in the integral

#### (a) $N(2\theta)$

The volume element cut out of the 'thick Ewald sphere' by an increment  $\Delta\theta\Delta\varphi$  is proportional to  $\sin^2(2\theta)/\lambda^3 \Delta\theta\Delta\varphi$  (Fig. 2); therefore,  $N(2\theta) \sim \sin^2(2\theta)/\lambda^3$ . The expression 'thick Ewald sphere' is used here to designate a range of Ewald spheres each corresponding to a given ray in the incident beam having a beam divergence  $\delta$ . It is not necessary to consider absolute intensities; therefore, scale effects arising from the crystal volume, the beam divergence, the cell volume and the average pathlength need not be considered. However, the dependence of the phenomenon on the wavelength is of interest.

#### (b) $r_{02}(2\theta, \varphi)$

For the purposes of the present analysis, it is adequate to consider that all reflections at a given  $2\theta$  angle have the same structure factor value  $|F(2\theta)| = c e^{-k \sin^2 \theta/\lambda^2}$ . The parameter  $k$  allows for the thermal motion of the atoms and the  $2\theta$  dependence of the average scattering curve. Experimentally, one finds that  $\langle F_o(2\theta) \rangle$  follows this law reasonably well (see *Experimental*). Many reflections contribute to the *Umweganregung* of a given reflection and the above simplification assumes that the resulting average effect is the

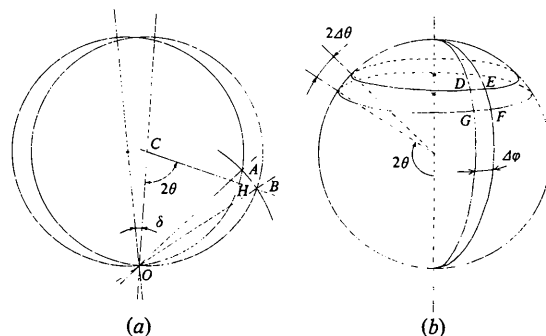


Fig. 2. (a) Thickness  $BH$  of the Ewald sphere at a given  $2\theta$  angle:  $CB$  is a radius of the Ewald sphere of an extreme ray in the beam divergence  $\delta$ ;  $AB$  is a circular arc with center  $O$ ; the angle  $AOB$  is equal to  $\delta$ ; the length of the arc  $AB$  is  $2\delta \sin \theta/\lambda$ . For small  $\delta$ ,  $BH \sim AB \cos \theta$ , or  $\delta \sin 2\theta/\lambda$ . (b) Area determined by a  $\Delta\theta\Delta\varphi$  increment about the  $2\theta, \varphi$  direction:  $DG = EF = 2\Delta\theta/\lambda$ ;  $DE \sim GF \sim \sin 2\theta/\lambda \Delta\varphi$ ; consequently, the area  $EDFG$  is equal to  $2 \sin 2\theta/\lambda^2 \Delta\theta\Delta\varphi$ . Combining the two results, the volume element cut out of the 'thick Ewald sphere' by a  $\Delta\theta\Delta\varphi$  increment is  $2\delta \sin^2 2\theta/\lambda^3 \Delta\theta\Delta\varphi$ .

same as would be produced by average reflections. This holds for compounds where the repartition of atoms can be considered to be random. If this is not the case (e.g. when a heavy atom is in a rational position) subsets of the intensities would have to be considered separately.

If the beam divergence is larger than the crystal mosaic, we satisfy the conditions for peak top intensity measurement where no motion is applied to the crystal and where the maximum reflected intensity is proportional to the integrated intensity giving:

$$r_{02} = (c_1 \lambda^3 P_{02} / \sin 2\theta) e^{-2k \sin^2 \theta / \lambda^2},$$

where  $c_1$  is a scale factor and  $P_{02}$  is the appropriate polarization factor.

(c)  $r_{21}(2\theta, \varphi)$

Each reflection (2) has a diffracted beam divergence governed by the mosaic spread. If the kinematical model of diffraction is assumed, the average reflectivity  $r_{21}$  while in reflection position is proportional to the integrated reflection, analogous to  $r_{02}$ ,

$$r_{21} = (c_2 \lambda^3 P_{21} / \sin 2\theta_{12}) e^{-2k \sin^2 \theta_{12} / \lambda^2},$$

where  $2\theta_{12}$  is the unoriented angle between the directions (1) and (2).

(d)  $t_{21}(2\theta, \varphi)$

The duration of the reflection condition is equal to the thickness at node 1 of the Ewald sphere due to the

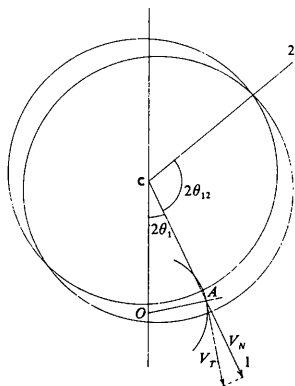


Fig. 3. Duration  $t_{21}$  of the 2→1 reflection condition. The speed  $V_N$  of node  $A$  normal to the Ewald sphere is its speed  $V_T$  tangential to its circular scan around  $O$  multiplied by the cosine of the angle  $\theta_1$  between  $V_T$  and  $V_N$ . The radius  $OA$  of the circular travel is  $2 \sin \theta_1 / \lambda$ . For a rotation speed  $\omega$ , the normal speed is  $\omega \sin 2\theta_1 / \lambda$ . Following the result in Fig. 2(a), the thickness of the Ewald sphere at  $A$  is  $\delta \sin 2\theta_{12} / \lambda$ , giving a reflection time  $t_{12}$  proportional to  $\sin 2\theta_{12} / \sin 2\theta_1$ . The beams 0, 1 and 2 are represented coplanar for ease of drawing, but the reasoning is the same if they are not coplanar.

divergence of beam (2) divided by the speed normal to the sphere  $V_N$  of node 1 in its motion about the origin  $O$  of the reciprocal lattice; therefore, it is proportional to  $\sin 2\theta_{12} / \sin 2\theta_1$  (Fig. 3) giving:

$$\Delta Q_1 = C \lambda^3 \int_{\theta, \varphi} (\sin 2\theta / \sin 2\theta_1) \times P_{021} e^{-2k(\sin^2 \theta + \sin^2 \theta_{12}) / \lambda^2} d\theta d\varphi.$$

where  $C$  is a scale factor and  $P_{021}$  is the polarization correction appropriate to the double reflection developed in Appendix I.

### Method

The above expression includes an unspecified scale factor  $C$  prohibiting the calculation of  $\Delta Q_1$ . However, its unscaled value,  $U(2\theta_1) = \Delta Q_1 / C \lambda^3$ , can be evaluated by numerical integration and then scaled to the experiment by comparison with the results of a least-squares refinement or by comparison with the measured intensities of the systematic extinctions when a sufficient number of them are present.

### Experimental

The intensities of quartz and epidote were measured using the profile-analysis method of the  $\theta$ - $2\theta$  scan of Grant & Gabe (1978) (Table 1). The refinement of the data using counting-statistics weights gave the residuals  $R = 0.93\%$ ,  $R_w = 1.63\%$  for quartz and  $R = 2.04\%$ ,  $R_w = 2.73\%$  for epidote. The analysis of both refinement results showed that the graph of  $\langle |F_c| \rangle / \langle F_o \rangle$  as a function of  $F_o$  was equal to 1.00 over most of the  $F_o$  range, but that it became very significantly less than 1.00 for small values of  $F_o$  indicating the overestimation of the weak intensities due to the probable presence of multiple reflections. The theoretical  $2\theta$  dependence of the multiple-reflection contribution to the measured intensity was then calculated in the following way. The plot of  $\ln \langle F_o \rangle$  as a function of  $\sin^2 \theta$  was approximately linear in accordance with the hypothesis that  $\langle F_o \rangle = c \exp(-k/\lambda^2 \sin^2 \theta)$ . The slope of the plot gave  $k/\lambda^2 = 3.2$  for quartz and 2.4 for epidote (Fig. 4). The knowledge of this parameter is sufficient to calculate the integral giving  $\Delta Q_1$  by numerical integration over the Ewald sphere, except for a small region surrounding beam (1) which does not correspond to a physically meaningful situation [reflection of beam (1) along beam (1)], giving the unscaled expected value of *Umweganregung*,  $U(2\theta_1)$ . This value was compared with the experiment by calculating  $S = \langle (I_{\text{obs}} - I_{\text{calc}}) / U(2\theta) \rangle$  for the weak reflections. The quantity  $S U(2\theta)$  is the expected number of extra counts per reflection due to *Umweganregung* at the given  $2\theta$  angle. This number of counts

(Fig. 5) was subtracted from each reflection. The average correction corresponds to 0.20% of the average diffracted intensity for quartz and 0.33% for epidote. The refinement using the corrected intensities and the same weights gave  $R = 0.89\%$  and  $R_w = 1.63\%$  for quartz and  $R = 1.91\%$  and  $R_w = 2.52\%$  for epidote. The plot of the re-scale factor as a function of  $F_o$  (Fig. 6) shows a considerable improvement for the small  $F_o$ . Quartz is noncentrosymmetric and has a small cell volume. Only about 25 Friedel pairs or 6% of the data have  $F_o/F_o(\text{max}) < 1/50$ . In epidote, which is centrosymmetric with a large cell, this number is about 700 or nearly 20% of the data. This fact is partly responsible for the smaller improvement of the residuals for quartz.

The inclusion of the multiple-reflection contribution in the weights by considering the average contribution as a proportion of its own  $\sigma$ , in a way that will be fully developed in a subsequent article on least-squares

weights, gives the residuals  $R = 0.78\%$  (0.83% including the unobserved reflections),  $R_w = 1.01\%$  (including the unobserved reflections) and  $R = 1.80\%$ ,  $R_w = 1.72\%$  for epidote.

### Conclusion

When using Mo radiation and compounds with small thermal motion, *Umweganregung* is a significant and systematic contributor to the weak reflection intensities. The  $2\theta$  dependence of its average contribution has been established from simple assumptions. Corrections of the intensities and the weights for this factor leads to a significant improvement of the refinement results. The

Table 1. *Refinement information*

	Quartz	Epidote		
Sample as in	Le Page (1978); Le Page & Gabe (1978)	Gabe, Portheine & Whitlow (1973)		
Space group	$P3_121$	$P2_1/m$		
$a$ (Å)	4.9134	8.8877 (14)		
$b$ (Å)		5.6275 (8)		
$c$ (Å)	5.4052	10.1517 (12)		
$\beta$ (°)		115.383 (14)		
Formula unit	$\text{SiO}_2$	$\text{Ca}_2\text{Al}_2(\text{Al,Fe})\text{Si}_3\text{O}_{13}\text{H}$		
$Z$	3	2		
Radiation and range	Mo $K\alpha$ , $2\theta \leq 90^\circ$	Mo $K\alpha$ , $2\theta \leq 90^\circ$		
Intensity measurement method	Profile analysis of $\theta/2\theta$ scan ( $\sim 1$ min/reflection)			
Independent reflections	629	4055		
Observed reflections [ $\geq 2\sigma(I)$ ]	615	3855		
Symmetrically related sets measured	6	1		
Least-squares parameters	17	130		
	Residuals on all observed reflections (%)			
	$R$	$R_w$	$R$	$R_w$
Standard refinement	0.93	1.63	2.04	2.73
<i>Umweganregung</i> subtracted from intensities	0.89	1.63	1.91	2.52
<i>Umweganregung</i> subtracted from intensities and allowed for in weights	0.78	1.01	1.80	1.72
Scattering curves	Non-ionized atoms (RHF) from <i>International Tables for X-ray Crystallography</i> (1974)			

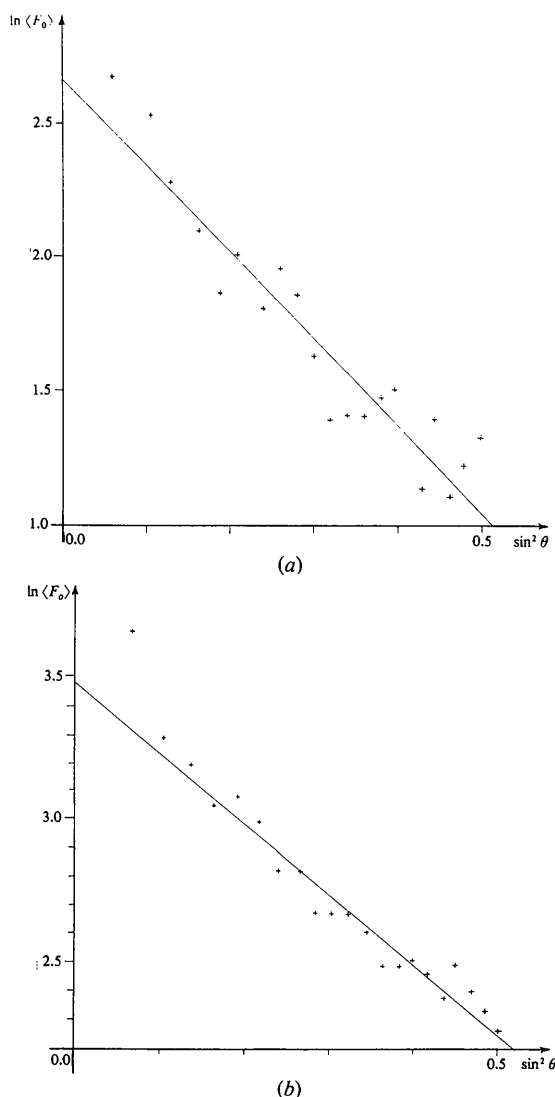


Fig. 4. Plot of  $\ln \langle F_o \rangle$  versus  $\sin^2 \theta$  to obtain the parameter  $k/\lambda^2$  when it is assumed that  $F_o = C \exp(-k/\lambda^2 \sin^2 \theta)$ . (a) Quartz, (b) epidote.

present treatment focuses on X-rays, though similar problems are met in neutron intensities (for example, see Thompson & Grimes, 1977) and the present approach would be applicable to neutron intensity measurements.

We wish to thank Dr L. D. Calvert for his continued interest in this work.

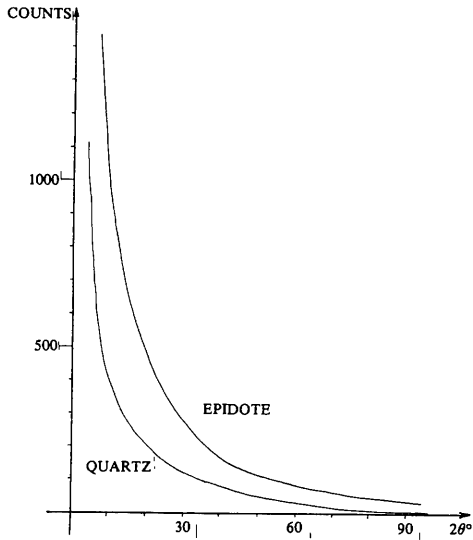


Fig. 5. Extra counts per reflection due to *Umweganregung* versus  $2\theta$  for quartz and epidote. The curves shown are the theoretical curves scaled to the experiment by analysis of the least-squares results. The quartz curve decreases faster with increasing  $2\theta$  angle owing to the larger thermal motion in this compound.

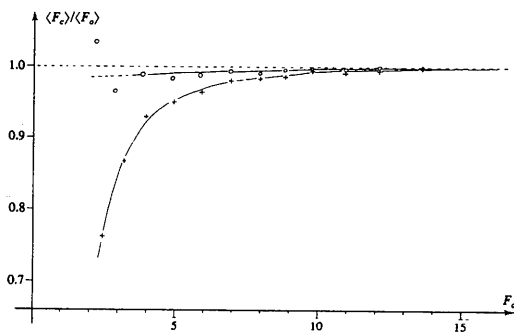


Fig. 6.  $\langle F_c \rangle / \langle F_o \rangle$  as a function of  $F_o$  before (crosses) and after (circles) correction for epidote. The maximum  $F_o$  is 242 and the plotted quantity is  $1.000 \pm 6$  for  $F_o$  over 15. Each point corresponds to the averaging of 190 reflections. The similar plot for quartz shows essentially one discrepant point at about 0.9 due to the comparatively smaller number of weak reflections in non-centrosymmetric compounds.

## APPENDIX

### The polarization correction for multiple reflection

Assuming an unpolarized incident beam of amplitude  $E$  propagating along the  $+X$  direction in a Cartesian reference system  $XYZ$  (Fig. 7a), we define two diffraction directions: direction (1) in the  $XZ$  plane with spherical coordinates  $(2\theta_1, 0)$  and therefore direction cosines  $(\cos 2\theta_1, 0, \sin 2\theta_1)$  in position for intensity measurement, and direction (2) with coordinates  $(2\theta, \varphi)$  and direction cosines  $(\cos 2\theta, -\sin 2\theta \sin \varphi, \sin 2\theta \cos \varphi)$ . In order to calculate the polarization for the double reflection  $0 \rightarrow 2 \rightarrow 1$ , we perform the following rotations of the reference system.

#### Rotation A

The  $XYZ$  axes are transformed to  $X_A Y_A Z_A$  (Fig. 7a) by a rotation by an angle  $\varphi$  about  $X$ . The rotation matrix is

$$\begin{bmatrix} 1 & 0 & 0 \\ 0 & \cos \varphi & \sin \varphi \\ 0 & -\sin \varphi & \cos \varphi \end{bmatrix}.$$

Beam (2) is in the  $X_A Z_A$  plane with spherical coordinates  $(2\theta, 0)$  and direction cosines  $(\cos 2\theta, 0, \sin 2\theta)$  while beam (1) has coordinates  $(2\theta_1, -\varphi)$  and direction cosines  $(\cos 2\theta_1, \sin 2\theta_1 \sin \varphi, \sin 2\theta_1 \cos \varphi)$ .

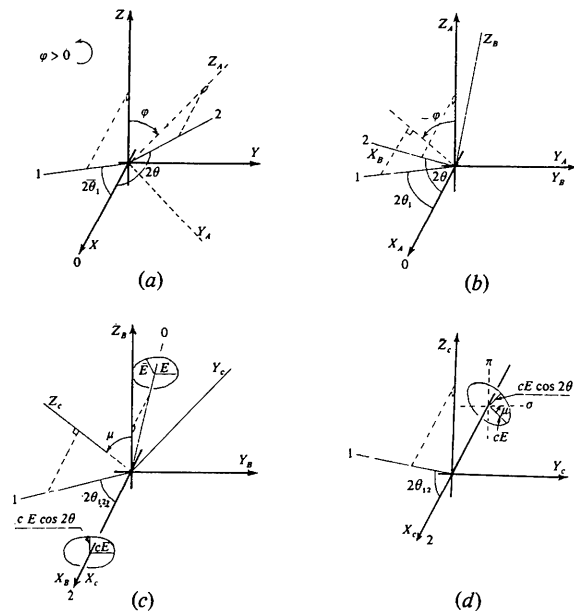


Fig. 7. Rotations of the reference system for the calculation of the polarization of the double reflection  $0 \rightarrow 2 \rightarrow 1$ .

**Rotation B**

Rotation by an angle  $2\theta$  about  $Y_A$  brings  $X_A$  into  $X_B$  along beam (2) (Fig. 7b). The rotation matrix is

$$\begin{bmatrix} \cos 2\theta & 0 & \sin 2\theta \\ 0 & 1 & 0 \\ -\sin 2\theta & 0 & \cos 2\theta \end{bmatrix}.$$

Beam (1) now has the direction cosines  $(\cos 2\theta_1 \cos 2\theta + \sin 2\theta_1 \sin 2\theta \cos \varphi, \sin 2\theta_1 \sin \varphi, \sin 2\theta_1 \cos 2\theta \cos \varphi - \cos 2\theta_1 \sin 2\theta)$ .

The principal vibration directions of beam (2) are along  $Y_B$  and  $Z_B$  and, if a mosaic crystal and no extinction are assumed, their amplitudes are respectively  $cE$  and  $cE \cos 2\theta$ , where  $c$  is a proportionality constant.

**Rotation C**

Rotation by an angle  $\mu$  about  $X_B$  brings  $Z_B$  into  $Z_C$  in the plane defined by  $X_B$  and the beam (1). The angle  $\mu$  is obtained from the direction cosines of beam (1) with  $Y_B$  and  $Z_B$  (Fig. 7c):

$$\begin{aligned} \tan \mu &= -\frac{\cos(1 \wedge Y_B)}{\cos(1 \wedge Z_B)} \\ &= \frac{\sin 2\theta_1 \sin \varphi}{\cos 2\theta_1 \sin 2\theta - \sin 2\theta_1 \cos 2\theta \cos \varphi}, \end{aligned}$$

and the rotation matrix is:

$$\begin{bmatrix} 1 & 0 & 0 \\ 0 & \cos \mu & \sin \mu \\ 0 & -\sin \mu & \cos \mu \end{bmatrix}.$$

*Acta Cryst.* (1979). **A35**, 78–82

**A Priori Estimates of Errors in Intensities for Imperfectly Spherical Crystals**

BY M. G. VINCENT AND H. D. FLACK

*Laboratoire de Cristallographie aux Rayons X, Université de Genève, 24 quai Ernest Ansermet, CH-1211 Genève 4, Switzerland*

(Received 27 May 1978; accepted 5 July 1978)

**Abstract**

*A priori* estimates of errors in intensities for spheres arising from non-sphericity in crystal shape may now be readily determined from a recently published table of  $(1/A^*)(\partial A^*/\partial \mu R)$  values [Flack & Vincent (1978). *Acta Cryst.* **A34**, 489–491] using an expression given

0567-7394/79/010078-05\$01.00

The direction cosines of beam (1) are  $(\cos 2\theta_{12}, 0, \sin 2\theta_{12})$  with  $\cos 2\theta_{12} = \cos(1 \wedge X_B) = \cos 2\theta_1 \cos 2\theta + \sin 2\theta_1 \sin 2\theta \cos \varphi$ . From Fig. 7(d) the radiation along beam (1) has two independent parallel components for the 2→1 reflection with amplitudes  $cE \cos \mu$  and  $cE \cos 2\theta \sin \mu$ . After reflection, the intensity with  $\sigma$  polarization is  $c_1^2 E^2 (\cos^2 \mu + \cos^2 2\theta \sin^2 \mu)$ . In the same way, the intensity with  $\pi$  polarization is  $c_1^2 E^2 \cos^2 2\theta_{12} (\cos^2 2\theta \cos^2 \mu + \sin^2 \mu)$ , where  $c_1$  is a proportionality constant.

Finally, the polarization correction appropriate to the 0→2→1 reflection is

$$\begin{aligned} P_{021} &= \frac{1}{2} [\cos^2 \mu + \cos^2 2\theta \sin^2 \mu + \cos^2 2\theta_{12} \\ &\quad \times (\cos^2 2\theta \cos^2 \mu + \sin^2 \mu)]. \end{aligned}$$

**References**

- COPPENS, P. (1968). *Acta Cryst.* **A24**, 253–257.  
 GABE, E. J., PORTHEINE, J. C. & WHITLOW, S. H. (1973). *Am. Mineral.* **58**, 218–223.  
 GRANT, D. F. & GABE, E. J. (1978). *J. Appl. Cryst.* **11**, 114–120.  
*International Tables for X-ray Crystallography* (1974). Vol. IV. Birmingham: Kynoch Press.  
 LE PAGE, Y. (1978). To be published.  
 LE PAGE, Y. & DONNAY, G. (1976). *Acta Cryst.* **B32**, 2456–2459.  
 LE PAGE, Y. & GABE, E. J. (1978). *J. Appl. Cryst.* **11**, 254–256.  
 MOON, R. M. & SCHULL, C. G. (1964). *Acta Cryst.* **17**, 805–812.  
 POST, B. (1969). *Acta Cryst.* **A25**, 94–95.  
 RENNINGER, M. (1937). *Z. Phys.* **106**, 141–176.  
 THOMPSON, P. & GRIMES, N. P. (1977). *J. Appl. Cryst.* **10**, 369–371.

by Jeffery & Rose [*Acta Cryst.* (1964), **17**, 343–350]. However, a new relationship between  $\sigma(R)$  and  $\sigma(r)$  is determined. The effects of crystal radius, non-sphericity and wavelength on intensity errors are discussed. The importance to the selection of crystals for electron density measurements is stressed. Universal curves of  $\sigma(r)/r$ , the error due to non-sphericity, against  $\mu r$  calcu-

©1979 International Union of Crystallography